Effect of hydrogenation on structure and superconducting properties of CaC$_6$

G. Srinivas,*[a] C. A. Howard,[a] S. M. Bennington,[b] N. T. Skipper[a] and M. Ellerby[a]

We report the effects of hydrogenation on the structure and superconducting properties of good quality bulk superconducting CaC$_6$ samples prepared from Madagascar graphite single crystals using a Ca-metal vapour transport method. The hydrogenation of a CaC$_6$ sample takes several hours during which, at different hydrogen exposure times, the structural and superconducting studies were carried out using X-ray diffraction, Raman scattering, and temperature and field dependence of magnetization measurements. These studies reveal that only a mixture of CaH$_2$ and graphite is obtained upon hydrogenation of CaC$_6$. The successive suppression of superconducting volume fraction and critical temperature is observed when increasing the hydrogenation time. The results reveal that there is a definite relation between structure and superconductivity in the hydrogenated CaC$_6$ samples. The changes in stoichiometry and inevitable Ca-sub-lattice disorder during the deintercalation process are considered to be the main sources for the change in the superconducting transition temperature.

1. Introduction

It is well known that some graphite intercalated compounds (GICs) are superconducting.[1–5] Superconductivity in GICs was first reported in 1965 in the potassium–graphite donor compound KC$_8$ with a transition temperature (T_C) of 0.14 K[6] Until the discovery of superconductivity in YbC$_6$ and CaC$_6$ at T_C = 6.5 K and 11.5 K respectively[3,4] (and higher at elevated pressures[7,8]), the highest transition temperatures observed in GICs were in KTl$_{1.5}$C$_4$ with a T_C of 2.7 K, synthesized at ambient pressure,[9] and in metastable NaC$_2$, with a T_C of 5 K, synthesized at high pressures.[10] The superconductivity in YbC$_6$ and CaC$_6$[3,4] has attracted a great deal of attention, and has stimulated a search for GICs with even higher transition temperatures by varying the chemical composition and/or the intercalant.[1,11]

Hydrogen is known to absorb in alkali-metal GICs. At ambient pressure the hydrogen chemisorption process depends on the alkali-metal species and the stage of intercalation (where a stage-n GIC has n graphene layers for every filled interlayer gallery).[12] For example, in potassium GICs hydrogen reacts most easily with stage-1 KC$_8$ to give stage-2 KC$_8$H$_{0.67}$ thereby producing a sandwich structure of triple-atomic planes, K–H–K along the c-axis. In contrast to this the caesium based GICs show very little affinity for hydrogen. In some GICs, such as K–Hg GICs, no changes in structure and c-axis repeat distance are observed as hydrogen is absorbed,[12] whereas in others the interaction can be large: in the stage-1 LiC$_6$ the strong interaction between the lithium and hydrogen draws the lithium from the GIC to leave graphite and LiH.[12,13]

Hydrogenation also has a large effect on the superconducting properties of GICs. The hydrogenation dependence of T_C in GICs was first studied in KC$_8$.[14] The partially hydrogenated compound KC$_8$H$_{0.19}$[15] showed a higher transition temperature and a broader transition than that of KC$_8$.[14,16] At the saturated hydrogen concentration in KC$_8$H$_{0.67}$, no superconductivity was observed down to 52 mK.[14] In contrast, a remarkable 80% increase in T_C and a narrowing of the transition was reported in hydrogenated stage-1 K–Hg GIC.[17] Recently an increase in the superconducting transition temperature was reported in a hydrogenated layered superconducting MgB$_2$ due to increased phonon frequency and a larger unit cell volume.[11,18] Clearly it is difficult to draw any general conclusions about the effect of hydrogen on the structure and superconductivity in GICs, just as it is with transition metals.

Here we present a systematic and detailed study on the effect of hydrogen on the structure and superconducting properties of CaC$_6$ using X-ray diffraction (XRD), Raman spectroscopy and the temperature and field dependence of magnetization measurements. To our knowledge, this is the first study on the hydrogenation properties of CaC$_6$.

It is known that the CaC$_6$ compounds synthesized using the molten Li–Ca alloy route have Li and Li–Ca alloy impurity phases.[4,19,20] These Li-based impurity phases are known to have lower transition temperatures than pure CaC$_6$[1] and may give rise to other spurious properties due to hydrogenation. Therefore the samples used in this work were prepared using a calcium vapour transport route. This method produces high purity Li free samples, but has in the past led to non-homogeneous materials with poor and irreproducible superconducting transitions.[3,21] In this work we were succeeded in producing high quality CaC$_6$ samples by vapour transport method using Madagascar graphite single crystals. The XRD and Raman studies reveal the development of a mixture of CaH$_2$ and graphite phases at the expense of the CaC$_6$ phase upon hydrogenation. The complete suppression of superconductivity is observed in the hydrogen saturated samples. The superconducting properties are discussed based on the observed experimental results and correlated with the structural changes upon hydrogenation.

[a]London Centre For Nanotechnology, University College London, 17–19 Gordon Street, London, UK, WC1H 0AH. E-mail: g.srinivas@ucl.ac.uk; Fax: +44 (0) 20 7679 0595; Tel: +44 (0) 20 7679 3526
[b]Rutherford Appleton Laboratory, Chilton, Didcot, UK, OX11 0QX

2. Experimental

The samples were prepared from previously out-gassed $\sim 2.0 \times 0.3$ mm Madagascar natural crystals and high purity calcium metal (99.99% from Sigma Aldrich). We used a vapour transport method[5] where the metal and graphite crystals were placed inside a sealed stainless steel tube in an argon glove box. The tube was then placed in a furnace and pumped to $<1.0 \times 10^{-7}$ mbar. Intercalation times varying from a week to several weeks were tried at several temperatures in the range 450–500 °C. The resulting CaC_6 samples were golden in colour. After characterising the pristine CaC_6, samples were exposed to 10 bar high purity hydrogen in a stainless steel reactor at temperatures between 25 and 500 °C. In order to avoid possible hydrogen desorption, the sample cell was cooled down to room temperature before the pressure was released. All the subsequent handling of the samples was in an argon filled glove box. The structure and phase identification of pristine and hydrogenated CaC_6 samples was made using powder XRD and Raman spectroscopy. The XRD measurements were performed at room temperature using an X'pert Pro, PANalytical diffractometer using Mo Kα radiation in inert atmospheric conditions. The Raman spectra were recorded with a ×50 microscope using a 514.5 nm Ar⁺ laser (Renishaw inVia Raman microscope) also at room temperature. The samples were set in a specially designed sample cell in a glove box in order to avoid exposure to oxygen and water vapour. Magnetization measurements as a function of temperature and field dependence were performed in a Quantum Design superconducting quantum interference device magnetometer (MPMS7), with the applied field perpendicular to the basal plane. The temperature dependence of the magnetization measurements has been carried out on both the zero field cooled (ZFC; where the samples were initially cooled to 2 K with the magnetic field switched off) and field cooled (FC) samples. The field dependent magnetization has been carried out on the ZFC samples.

3. Experimental results

Fig. 1 shows the XRD patterns of pristine and hydrogenated CaC_6 samples subjected to different exposure times at 500 °C under 10 bar hydrogen pressure. The pristine CaC_6 sample (Fig. 1) shows two sets of XRD reflections indicating two well defined phases: rhombohedral CaC_6 and unintercalated hexagonal graphite. The samples exposed to hydrogen at certain time scales with increasing order are shown in Fig. 1. With increasing hydrogen exposure time, the XRD patterns show the gradual disappearance of the CaC_6 phase and the growth of new phase corresponding to orthorhombic (space group: *Pnma*) CaH_2.[22] A comparison of the intensities, in particular for the 30 min hydrogenated sample shows a large decrease in the CaC_6 phase due to the growth of CaH_2. At higher hydrogenation times, the samples show only mixtures of CaH_2 and graphite with complete suppression of the CaC_6 phase. Furthermore, as the hydrogenation time increased, the samples show broadening of the 002 graphite reflections and a decrease in the intensity without appreciable change in its 2θ position. All the platelets of the pristine CaC_6 sample were initially shiny gold in colour but subsequently turn black after they have been exposed to hydrogen.
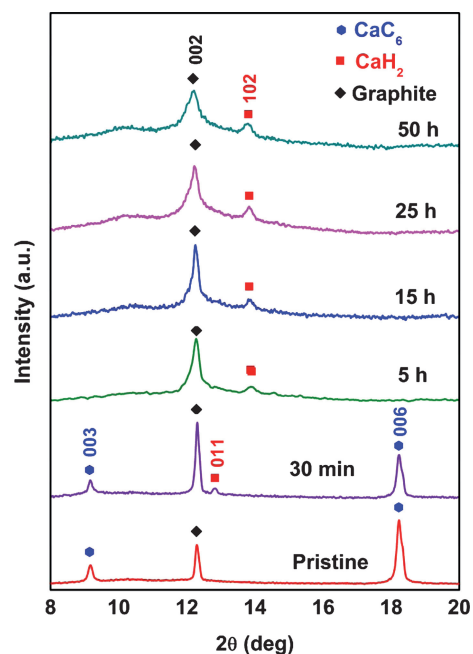

Fig. 1 The XRD patterns of pristine and hydrogenated CaC_6 samples; the samples subjected to different exposure times at 500 °C and 10 bar hydrogen pressure. The measurements were made in reflection using Mo Kα radiation.
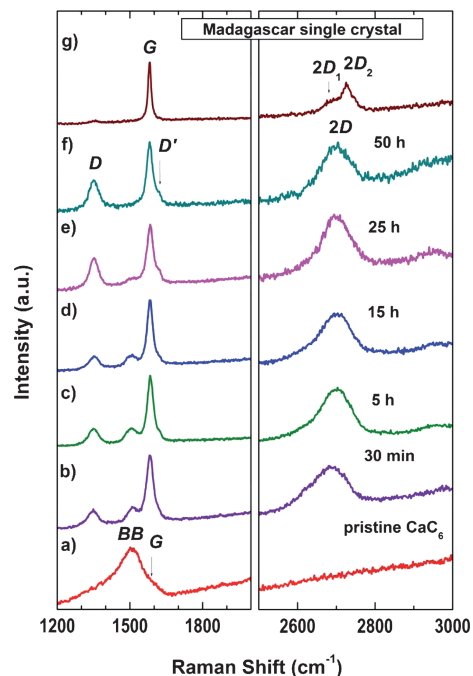

Fig. 2 The Raman spectra of pristine and hydrogenated CaC_6 samples; the samples subjected to different exposure times at 500 °C and 10 bar hydrogen pressure. The spectra were measured with 514.5 nm wavelength light.

Fig. 2 presents the Raman spectra for CaC_6 samples as a function of hydrogen exposure time along with constituent Madagascar single crystal graphite. The initial CaC_6 sample shows a strong asymmetric broadband (*BB*) near 1500 cm⁻¹

corresponding to the band stretching E_g mode along with a weak G band near 1580 cm^{-1} corresponding to the unintercalated graphite.[23] The BB (E_g mode) is a bond stretching mode of the graphene layer that is only active in intercalated graphite. As the hydrogenation progresses, the hydrogenated CaC$_6$ samples show the development of clear D, G, D' and $2D$ (overtone of the D band) bands near 1350 cm^{-1}, 1580 cm^{-1}, 1620 cm^{-1} and 2700 cm^{-1} respectively, relating to the hexagonal graphitic structure,[24] whilst the BB peak from the CaC$_6$ reduces in size and eventually disappears after 50 h exposure. The Raman spectra of the graphite produced in the hydrogenated CaC$_6$ samples differ significantly when compared to that of Madagascar single crystals. Specifically, the G band broadens without a shift in frequency and the D band grows in intensity. Furthermore, a significant change in shape of the second-order $2D$ band can be seen, where the two component structure is lost leaving a single broad peak.

Fig. 3 shows the temperature dependence of dc magnetization in zero field cooled at 50 and 200 Oe for c-axis oriented CaC$_6$ samples as a function of hydrogen exposure time. Unlike previously reported vapour grown samples synthesized from highly oriented pyrolytic graphite (HOPG),[3,21,25] our pristine CaC$_6$ shows a sharp single step transition with clear saturation of diamagnetism, with a superconducting transition temperature of $T_C = 11.6$ K [Fig. 3(b)] consistent with previous reports.[3,4] The hydrogenation leads to a decrease in diamagnetic signal strength in the superconducting state, which can also be seen clearly in Fig. 3 and 4. Further, the close observation of Fig. 3(d) and 3(e) and inset (a) of Fig. 4 at magnetic fields of 50, 200 and 100 Oe respectively, reveal broader superconducting transitions and a slight decrease in T_C while increasing the hydrogenation time. Fig. 3(c) shows the rapid decrease of diamagnetic signal strength with increasing the hydrogenation time at 2 K and 50 Oe. By the time the sample had been hydrogenated for 50 h it did not exhibit superconductivity at least down to 2 K. This decrease of the
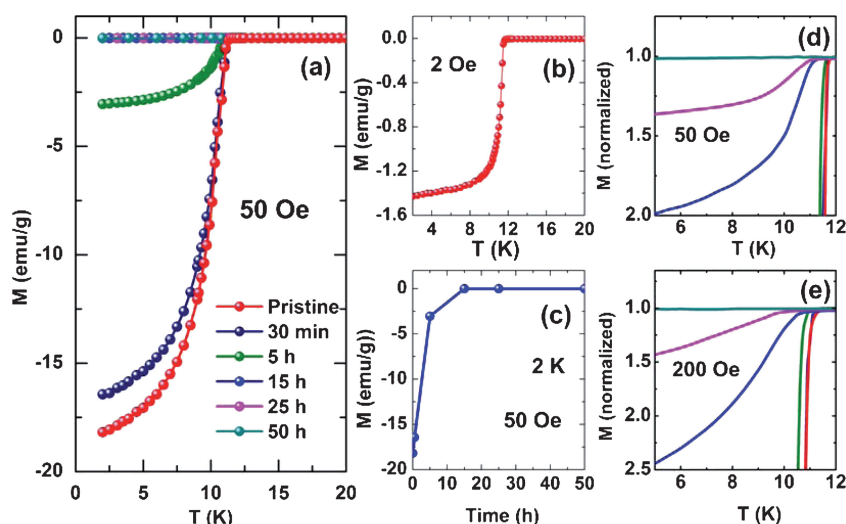

Fig. 4 The temperature dependent ZFC and FC magnetization of pristine and hydrogenated CaC$_6$ samples at an external applied field of 100 Oe. Inset (a) shows the clear variation of diamagnetic behaviour of very weak superconducting hydrogenated CaC$_6$ samples. Inset (b) shows the field dependent magnetization at 5 K for pristine and hydrogenated CaC$_6$ samples. The samples were subjected to different exposure times at 500 °C and 10 bar hydrogen pressure.

superconducting volume fraction upon increasing the hydrogen exposure time can be further clearly seen from the ZFC and FC dc magnetization plots (Fig. 4), where the width of the diamagnetic signal window continuously reduced. The reversible nature of the ZFC and FC magnetic signals can be seen in the 50 h hydrogenated sample as a function of temperature [Inset (a) of Fig. 4]. The inset (b) in Fig. 4 shows the hydrogenation and field

Fig. 3 The temperature dependent ZFC magnetization of pristine and hydrogenated CaC$_6$ samples at an external applied field of (a), (d) 50 Oe and (e) 200 Oe. (b) The step-like superconducting transition of the pristine CaC$_6$ sample at 2 Oe with clear saturation of diamagnetic signal in the superconducting state. (c) The variation of superconducting diamagnetic signal strength with increasing the hydrogenation time at 2 K and 50 Oe. (d), (e) Clear variation of T_C and diamagnetic behaviour at 50 Oe and 200 Oe respectively. The samples were subjected to different exposure times at 500 °C and 10 bar hydrogen pressure.
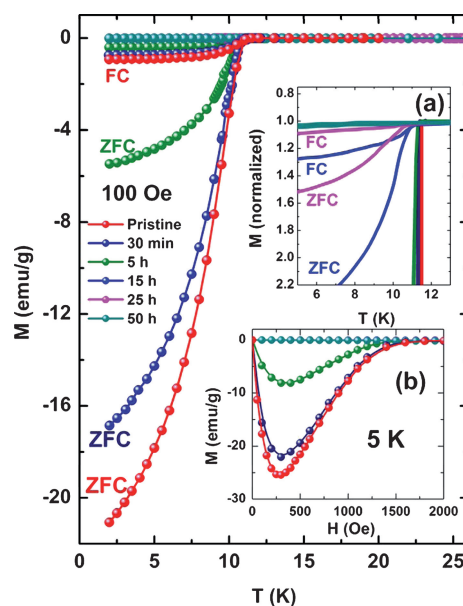
dependence of ZFC magnetization (M–H) plots measured at 5 K with the field oriented along the c-axis. The hydrogenation leads to a gradual suppression of the lower and upper critical fields (H_{C1} and H_{C2} respectively, defined as $M(H)$ minimum and zero crossing abscissas), both of which have reached zero after 50 h exposure to hydrogen.

4. Discussion

After a great deal of empirical testing, our best samples were produced using Madagascar flake graphite with calcium vapour. Our samples demonstrated a dominant CaC_6 phase (Fig. 1) compared to previously reported Ca-GICs made from HOPG.[3,21,25] The weight gain in our sample indicates that we obtain ~70% Ca-intercalation and that the CaC_6 phase is also evidenced from diffraction measurements. Further, the quality of our CaC_6 samples is clearly seen by the superconducting transition given in Fig. 3(b). The narrow single step-like transition and clear saturation of diamagnetic signal in the superconducting state is similar to that of "bulk" CaC_6 samples (at least 60% phase fraction) obtained from the molten Li–Ca alloy method.[4]

The XRD and Raman plots for the hydrogenated samples are shown in Fig. 1 and 2 and reveal only the development of the new orthorhombic CaH_2 phase[22] and an increase in the graphite volume fraction at the expense of the CaC_6 phase. Complete deintercalation takes place after 50 h of hydrogenation, after which time only graphite and CaH_2 remain. This effect is identical to that seen when LiC_6 is exposed to hydrogen, leading to deintercalation of Li and the formation of LiH and graphite,[12,13] which was attributed to the strong electron affinity of hydrogen towards lithium.[12] Clearly the availability of electronic charge on the donor intercalated metal and enthalpy of formation for metal hydrides play a major role in the structural transition of the hydrogenated GICs. For example, the charge transferred to the graphene layer and the magnitude of the enthalpy of formation of metal hydrides are lower in stage-1 KC_8 compared to a stage-1 LiC_6.[26,27] Thus, in stage-1 KC_8 the potassium remains intercalated in graphite and the hydrogen uptake leads to a full-scale structural transition to an ordered second stage compound $KC_8H_{2/3}$.[12] In CaC_6, Emery et al.[4] have reported the highest electron charge transfer between calcium and the graphene layer, 0.106 electrons per carbon atom, which is very high compared to 0.07 electrons per carbon atom in LiC_6.[28] Furthermore, the enthalpy of formation of CaH_2 (-180 kJ mol^{-1}) is twice that of LiH (-90.6 kJ mol^{-1}) and even three times that of KH (-58 kJ mol^{-1}).[27] Hydrogenation at significantly elevated temperatures also provokes the phase separation because the Ca atoms can move rapidly and rearrangement of Ca atoms can occur with respect to the graphene planes to reduce the total free energy of the compound. Therefore the absorbed hydrogen atoms prefer to interact directly with Ca. Thus the CaC_6 phase is no longer stable in the hydrogenated GIC, and a stable CaH_2 precipitates as happens in some of the hydrogenated intermetallics containing stable hydride forming elements.[29,30]

The much broader and weaker (002) graphite XRD reflection in the hydrogenated samples is attributed to a high degree of induced stacking disorder due to the deintercalation of Ca. The graphene layer separation in CaC_6 is 4.524 Å compared to 3.335 Å in high quality graphite. Presumably this large difference must

introduce high strains in the material creating a high degree of stacking disorder as the intercalant is extracted from the GIC. A similar disorder has been observed in deintercalated K-GICs,[31] where the authors suggest that the stages during deintercalation partially coexist, and this overlap creates greater strain. Furthermore, the development of disordered graphite in the hydrogenated CaC_6 samples is most clearly seen by comparing Raman bands to that of the constituent Madagascar single crystal (Fig. 2). The original crystals have the usual prominent G peak at 1580 cm^{-1} and very little evidence of any defect bands. It also has two peaks, $2D_1$ and $2D_2$, behaviour of a second-order $2D$ band around 2700 cm^{-1} associated with well ordered crystalline graphite.[24,32] Once hydrogenation starts the BB peak of the CaC_6 begins to disappear and is replaced by the spectra of more damaged graphite with a much broader G peak and prominent defect peaks, both D at 1350 cm^{-1} and D' at 1620 cm^{-1}. A universal observation is that the increase in disorder in graphite leads to a broader G band, as well as a broad D band of increased intensity. In particular the $2D$ band gives the structural parameters along the c-axis, since it is very sensitive to the stacking order of the graphene sheets along the c-axis.[24,33–35] The single peak behaviour of the second-order Raman band near 2700 cm^{-1} in all the hydrogenated CaC_6 samples is a sign of the total lack of c-axis order, and is observed in the most poorly organized materials (i.e., turbostratic graphite, without AB stacking).[32,34,35] Thus both the Raman and X-ray data demonstrate the violence of the deintercalation process, showing that not only is the graphite layering destroyed, the integrity of the basal plane is also disrupted. One further feature of the Raman measurements that should be noted is the absence of any C–H stretching modes around 2800–3000 cm^{-1}.[36] This confirms the atomic hydrogen is preferentially bound to the calcium and not to the graphite.

The decreased diamagnetic signal strength of CaC_6 samples with increasing hydrogenation time is almost certainly due to a reduction in the volume fraction of the CaC_6 phase as was also observed in the X-ray and Raman data. It is very clear that there is no superconducting transition in the completely hydrogenated (50 h) sample. However, the partially hydrogenated samples exhibit broader superconducting transitions as well as a decrease in T_C. The broader transitions can be often seen in non-homogeneous systems,[3] since the transition width depends more on the flux pinning properties of the samples. Since hydrogenation usually proceeds from the surface of a material, where most of the reactions nucleate at defects or grain boundaries (or micro-cracks in the case of a metal hydride system), in the hydrogenated system the fraction of remaining superconducting phases are separated by large regions of normal conducting or insulating material, CaH_2, similar to the granular superconducting systems.[37] Furthermore, much experimental information has accumulated over the years which shows that, though small amounts of disorder can either increase or decrease T_C, sufficiently large disorder will always destroy superconductivity. On the other hand, the discussions on the superconductivity in K-GICs have been greatly complicated by widely varying values reported for the T_C. Structural and stoichiometric distinctions among samples have been cited as the source of variation. Most importantly, T_C was observed to increase with increasing alkali-metal concentration.[10,38] Thus the partially hydrogenated CaC_6 samples might possess an in-plane Ca order or they may be

non-stoichiometric. One of the most important questions, however, is still not clear in Ca-GICs: what is the effect of stoichiometry and the in-plane arrangement of the intercalated Ca atoms on the T_C? In order to be able to guide interpretation and thereby gain some insight into the underlying superconducting mechanisms in these compounds, it is most important to understand the relationship between Ca stoichiometry, defect Ca ordering and structure, and T_C. It was reported that the intercalant disorder in the Ca-GICs leads to a decrease in T_C.[7,8,39] Indeed, the increased T_C and the transition narrowing seen in K–Hg GICs upon hydrogenation is attributed to the greater intercalant uniformity, caused by hydrogen diffusion into mercury vacancies associated with disorder.[17] Furthermore, the superconductivity in alkali-earth GICs is thought to be phonon mediated, the relevant phonons being C vibrations perpendicular and Ca vibrations parallel with the graphite planes.[1,23,40] The changes in Ca content and disordering may affect the lattice vibrational spectrum and therefore phonon interactions compared to pure CaC_6. It would be certainly very interesting to perform theoretical calculations on the non-stoichiometric and Ca defective CaC_6 and its effect on the T_C.

5. Conclusion

We have successfully synthesized the largest percent of Ca-intercalated GIC, from platelet-shaped single crystals of Madagascar natural graphite, which is the highest quality sample obtained to date using a vapour transport method. We have reported the first hydrogenation studies and the effect on the superconducting state of high quality bulk CaC_6 samples. The initial CaC_6 samples are golden in colour and change to black at higher hydrogenation times. The hydrogenation shows neither sign of restaging to higher stage compounds nor formation of ternary GICs, and generates only the mixture of disordered graphite and CaH_2 at the expense of the CaC_6 phase. Suppression of the superconductivity of CaC_6 upon increasing the hydrogenation time is attributed to the decrease in superconducting CaC_6 phase volume fraction. The broader and decreased superconducting transitions in partially hydrogenated samples are attributed to the increase in disorder caused by the deintercalation of Ca. No C–H bonding was observed in the hydrogenated CaC_6.

Acknowledgements

References

1 N. Emery, C. Herold, J.-F. Marache and P. Lagrange, *Sci. Technol. Adv. Mater.*, 2008, **9**, 044102.
2 J. S. Kim, L. Boeri, J. R. O'Brien, F. S. Razavi and R. K. Kremer, *Phys. Rev. Lett.*, 2007, **99**, 027001.
3 T. E. Weller, M. Ellerby, S. S. Saxena, R. P. Smith and N. T. Skipper, *Nat. Phys.*, 2005, **1**, 39.
4 N. Emery, C. Herold, M. d'Astuto, V. Garcia, C. Bellin, J. F. Mareche, P. Lagrange and G. Loupias, *Phys. Rev. Lett.*, 2005, **95**, 087003.
5 T. Enoki, M. Suzuki and M. Endo, *Graphite Intercalation Compounds and Applications*, Oxford University Press, Oxford, 2003.
6 N. B. Hannay, T. H. Geballe, B. T. Matthias, K. Andres, P. Schmidt and D. MacNair, *Phys. Rev. Lett.*, 1965, **14**, 225.
7 A. Gauzzi, N. Bendiab, M. d'Astuto, B. Canny, M. Calandra, F. Mauri, G. Loupias, N. Emery, C. Herold, P. Lagrange, M. Hanfland and M. Mezouar, *Phys. Rev. B*, 2008, **78**, 064506.
8 A. Gauzzi, S. Takashima, N. Takeshita, C. Terakura, H. Takagi, N. Emery, C. Herold, P. Lagrange and G. Loupias, *Phys. Rev. Lett.*, 2007, **98**, 067002.
9 R. A. Wachnik, L. A. Pendrys, F. L. Vogel and P. Lagrange, *Solid State Commun.*, 1982, **43**, 5.
10 I. T. Belash, A. D. Bronnikov, O. V. Zharikov and A. V. Palnichenko, *Synth. Met.*, 1990, **36**, 283.
11 W. X. Li, Y. Li, R. H. Chen, R. Zeng, S. X. Dou, M. Y. Zhu and H. M. Jin, *Phys. Rev. B*, 2008, **77**, 094517.
12 T. Enoki, S. Miyajima, M. Sano and H. Inokuchi, *J. Mater. Res.*, 1990, **5**, 435.
13 W. Ishida, H. Miyaoka, T. Ichikawa and Y. Kojima, *Carbon*, 2008, **46**, 1628.
14 M. Sano, H. Inokuchi, M. Kobayashi, S. Kaneiwa and I. Tsujikawa, *J. Chem. Phys.*, 1980, **72**, 3840.
15 S. Kaneiwa, M. Kobayashi and I. Tsujikawa, *J. Phys. Soc. Jpn.*, 1982, **51**, 2375.
16 Y. Koike, H. Suematsu, K. Higuchi and S. Tanuma, *Solid State Commun.*, 1978, **27**, 623.
17 G. Roth, A. Chaiken, T. Enoki, N. C. Yeh, G. Dresselhaus and P. M. Tedrow, *Phys. Rev. B*, 1985, **32**, 533.
18 Y. Nakamori, S. Orimo, T. Ekino and H. Fujii, *J. Alloys Compd.*, 2002, **335**, L21.
19 S. Pruvost, C. Herold, A. Herold and P. Lagrange, *Carbon*, 2004, **42**, 1825.
20 N. Emery, S. Pruvost, C. Herold and P. Lagrange, *J. Phys. Chem. Solids*, 2006, **67**, 1137.
21 D. G. Hinks, D. Rosenmann, H. Claus, M. S. Bailey and J. D. Jorgensen, *Phys. Rev. B*, 2007, **75**, 014509.
22 J. Bergsma and B. O. Loopstra, *Acta Crystallogr.*, 1962, **15**, 92.
23 J. Hlinka, I. Gregora, J. Pokorny, C. Herold, N. Emery, J. F. Mareche and P. Lagrange, *Phys. Rev. B*, 2007, **76**, 144512.
24 M. A. Pimenta, G. Dresselhaus, M. S. Dresselhaus, L. G. Cancado, A. Jorio and R. Saito, *Phys. Chem. Chem. Phys.*, 2007, **9**, 1276.
25 M. Ellerby, T. E. Weller, S. S. Saxena, R. P. Smith and N. T. Skipper, *Physica B*, 2006, **378–380**, 636.
26 L. Pietronero and S. Strassler, *Phys. Rev. Lett.*, 1981, **47**, 593.
27 A. Klaveness, H. Fjellvag, A. Kjekshus, P. Ravindran and O. Swang, *J. Alloys Compd.*, 2009, **469**, 617.
28 S. Pruvost, C. Herold, A. Herold and P. Legrange, *Carbon*, 2003, **41**, 1281.
29 M. P. Sridhar Kumar, B. Viswanathan, C. S. Swamy and V. Srinivasan, *Mater. Chem. Phys.*, 1988, **20**, 245.
30 G. Srinivas, V. Sankaranarayanan and S. Ramaprabhu, *J. Phys.: Condens. Matter*, 2008, **20**, 255224.
31 W.-C. Oh, S.-J. Cho and Y.-S. Ko, *Carbon*, 1996, **34**, 209.
32 H. Wilhelm, M. Lelaurain and E. McRae, *J. Appl. Phys.*, 1998, **84**, 6552.
33 R. J. Nemanich and S. A. Solin, *Solid State Commun.*, 1977, **23**, 417.
34 R. J. Nemanich and S. A. Solin, *Phys. Rev. B*, 1979, **20**, 392.
35 P. Lespade, A. Marchand, M. Couzi and F. Cruege, *Carbon*, 1984, **22**, 375.
36 N. Ogita, K. Yamamoto, C. Hayashi, T. Matsushima, S. Orimo, T. Ichikawa, H. Fujii and M. Udagawa, *J. Phys. Soc. Jpn.*, 2004, **73**, 553.
37 D. Belitz and T. R. Kirkpatrick, *Rev. Mod. Phys.*, 1994, **66**, 261.
38 R. A. Jishi and M. S. Dresselhaus, *Phys. Rev. B*, 1992, **45**, 12465.
39 S. Nakamae, A. Gauzzi, F. Ladieu, D. L'Hote, N. Emery, C. Herold, J. F. Mareche, P. Lagrange and G. Loupias, *Solid State Commun.*, 2008, **145**, 493.
40 M. Calandra and F. Mauri, *Phys. Rev. Lett.*, 2005, **95**, 237002.

This journal is © The Royal Society of Chemistry 2009

J. Mater. Chem., 2009, **19**, 5239–5243 | 5243